

PHOTODETACHMENT SPECTROSCOPY OF NEGATIVE CLUSTER IONS

Kit H. Bowen and Joseph G. Eaton
Department of Chemistry
The Johns Hopkins University
Baltimore, MD 21218, USA

ABSTRACT

Negative ion photoelectron spectra have been obtained for a variety of gas-phase cluster anions using visible photons. The negative cluster ions were generated by injecting relatively low energy electrons directly into the high density portion of an expanding supersonic jet. The spectra of $\text{NO}^-(\text{N}_2\text{O})_{n=1,2}$, $\text{H}^-(\text{NH}_3)_{n=1,2}$, $\text{NH}_2^-(\text{NH}_3)_{n=1,2}$, $\text{NO}^-(\text{Ar})_1$, $\text{NO}^-(\text{Kr})_1$, $\text{NO}^-(\text{Xe})_1$, $\text{O}_2^-(\text{Ar})_1$, $(\text{N}_2\text{O})_2^-$, and $(\text{CS}_2)_2^-$ reveal that they are simple ion-molecule complexes in which the excess negative charges are largely localized on sub-ions within the larger cluster anions. In addition to information on the bonding of cluster ions, the spectra also provide electron affinities and ion-solvent dissociation energies as a function of cluster size. The spectra of $(\text{CO}_2)_2^-$, $(\text{SO}_2)_2^-$, and $(\text{NO})_2^-$, on the other hand, indicate that these species are more complicated cases, and that they are not well described as simple ion-molecule complexes. Also, in the case of NH_4^- , evidence is found not only for the ion-molecule complex, $\text{H}^-(\text{NH}_3)_1$, but also for a higher energy isomer of tetrahedral geometry. Other systems studied include negative cluster ions of water and alkali metal cluster anions. Even though H_2O^- is unstable, clusters of water are able to bind an electron to form $(\text{H}_2\text{O})_n^-$. The spectra of $(\text{H}_2\text{O})_{n=2,6,7,10-17,19}^-$ and $\text{Ar}(\text{H}_2\text{O})_{n=2,6,7}^-$ provide the vertical detachment energies for these species. The alkali metals are the simplest of metals. The spectra of Na_{2-5}^- , K_{2-8}^- , Rb_{2-4}^- , and $\text{Cs}_{2,3}^-$ yield electron affinities as a function of cluster size as well as the electronic state splittings for neutral alkali metal clusters.

INTRODUCTION

The study of clusters affords an opportunity for a better understanding of the condensed phase at the microscopic level. Investigations of cluster ions provide an avenue for exploring ion solvation on a molecular scale. Negatively-charged cluster ions have analogs among solvated anions and excess electron states in solution. Here, we report the application of negative ion photoelectron (electron photodetachment) spectroscopy to the study of size-selected negative cluster ions.

Our goals in studying the photodetachment of negative cluster ions are (1) to explore their energetic properties as a function of cluster size and (2) to develop a descriptive understanding of the bonding within negative cluster ions. Important energetic properties include electron affinities and step-wise ion-solvent dissociation (solvation) energies. Clustering can be expected to stabilize the excess charge on negative ions. One also expects that electron affinity values will increase rapidly with cluster size for small clusters and then approach a limiting value at some larger size as the mean number of solvent molecules interacting with the anion becomes constant. Step-wise solvation energies should eventually decrease with increasing solvation numbers. The experiments reported here map out both electron affinities and step-wise solvation energies as a function of cluster size.

An important aspect of ion-neutral bonding concerns the distribution of excess negative charge over the negative cluster ion. One can imagine two extreme charge distribution categories where in one the excess charge is localized on a single component of the cluster ion, and where in the other there is a dispersal of the negative charge over part or all of the cluster ion. The situation where the excess charge is localized on a single component of the cluster ion is reminiscent of the usual notion of a solvated anion in which a central negative ion is surrounded by a sheath of neutral solvent molecules. There the central negative ion may be thought of as remaining largely intact even though it is perturbed by its solvents. In this case electrostatic interactions between the ion and the solvent molecules presumably dominate the bonding. In other cases, however, charge dispersal effects may also make significant contributions to the bonding. These contributions may arise either in the sense of covalency in ion-neutral bonds or in the sense of excess electron delocalization via electron tunneling between energetically and structurally equivalent sites within the cluster ion. In favorable cases the photoelectron spectra of negative cluster ions can offer clues as to

the nature of the excess charge distribution in these species.

In this paper the results are organized into two parts;

(1) ion-molecule complexes where the excess electron is localized on one component of the negative cluster ion, and (2) more complicated cluster anions involving significant excess negative charge dispersal. The spectra of $\text{NO}^-(\text{N}_2\text{O})_{n=1,2}$, $\text{H}^-(\text{NH}_3)_{n=1,2}$, $\text{NH}_2^-(\text{NH}_3)_{n=1,2}$, $\text{NO}^-(\text{Ar})_1$, $\text{NO}^-(\text{Kr})_1$, $\text{NO}^-(\text{Xe})_1$, $\text{O}_2^-(\text{Ar})_1$, $(\text{N}_2\text{O})_2^-$, and $(\text{CS}_2)_2^-$ reveal that they are simple ion-molecule complexes in which the excess negative charges are largely localized on sub-ions within the larger cluster anions. The spectra of $(\text{CO}_2)_2^-$, $(\text{SO}_2)_2^-$, and $(\text{NO})_2^-$, on the other hand, indicate that these species are more complicated cases, and that they are not well described as simple ion-molecule complexes. Also, in the case of NH_4^- , evidence is found not only for the ion-molecule complex, $\text{H}^-(\text{NH}_3)_1$, but also for a higher energy isomer of tetrahedral geometry. Other systems studied include negative cluster ions of water and alkali metal cluster anions. The spectra of $(\text{H}_2\text{O})_{n=2,6,7,10-17,19}^-$ and $\text{Ar}(\text{H}_2\text{O})_{n=2,6,7}^-$ provide the vertical detachment energies for these species. The spectra of Na_{2-5}^- , K_{2-8}^- , Rb_{2-4}^- , and $\text{Cs}_{2,3}^-$ yield electron affinities as a function of cluster size as well as the electronic state splittings for neutral alkali metal clusters.

EXPERIMENTAL

Negative ion photoelectron spectroscopy is conducted by crossing a mass-selected beam of negative ions with a fixed-frequency photon beam and energy analyzing the resultant photodetached electrons. Subtraction of the center-of-mass electron kinetic energy of an observed spectral feature from the photon energy gives the transition energy (the electron binding energy) from an occupied level in the negative ion to an energetically accessible level in the corresponding neutral. Our negative ion photoelectron spectrometer has been described previously.¹ It is comprised of three main component systems. These are (a) the beam line along which negative ions are formed, transported, and mass-selected, (b) the high-power argon ion laser operated intracavity in the ion-photon interaction region, and (c) the doubly magnetically shielded, high resolution hemispherical electron energy analyzer which is located below the plane of the crossed ion and photon beams. The mass selector is a cooled Colutron 600B Wien filter. This is a $E \times B$ velocity filter with electrostatic shims which compensate for the focusing effects of simple Wien filters. Mass selection allows us to "purify" our starting

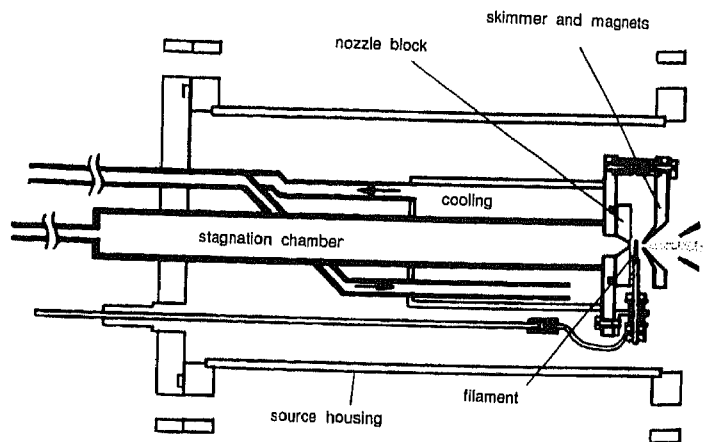


FIG. 1 Diagram of the supersonic expansion-ion source used in most of these experiments.

sample of negative ions before photodetachment and thus to obtain interference-free photoelectron spectra of specific negative ions. This capability is well suited for studies of homologous series of ions such as negative cluster ions.

Beams of negative cluster ions were generated in a supersonic expansion-ion source similar in spirit to that developed by Haberland.² Figure 1 presents a schematic of our version of this source. In this source a biased filament located just outside the nozzle orifice injects relatively low energy electrons into the supersonic expansion. Permanent magnets placed near the expansion jet were found to enhance the production of negative ions.

RESULTS AND DISCUSSION

Ion-Molecule Complexes: Cluster anions with localized excess negative charges

$\text{NO}^-(\text{N}_2\text{O})_{n=1,2}$ The photoelectron (photodetachment) spectra of the gas-phase negative cluster ions, $\text{NO}^-(\text{N}_2\text{O})_1$ and $\text{NO}^-(\text{N}_2\text{O})_2$ were recorded using 2.540 eV photons.³ Both spectra exhibit structured photoelectron spectral patterns which strongly resemble that of free NO^- , but which are shifted to successively lower electron kinetic energies with their individual peaks broadened (see Figure 2). Each of these spectra is interpreted in terms of a largely intact NO^- sub-ion which is solvated

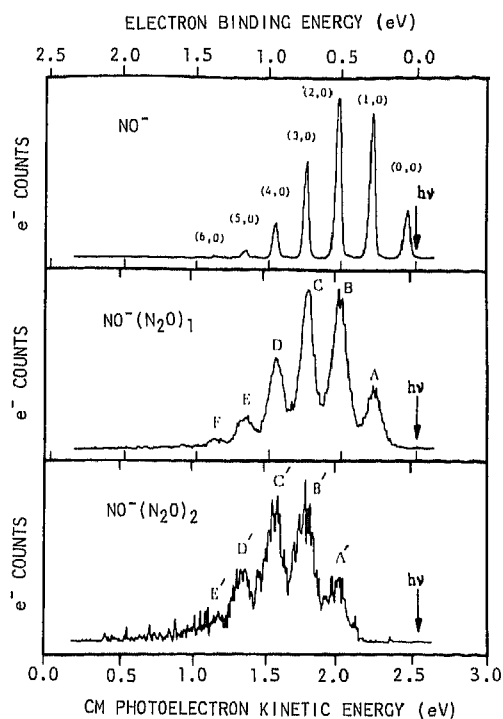


FIG. 2 The negative ion photoelectron spectra of NO^- , $\text{NO}^-(\text{N}_2\text{O})_1$, and $\text{NO}^-(\text{N}_2\text{O})_2$ all presented on the same center-of-mass electron kinetic energy and electron binding energy scales.

and stabilized by nitrous oxide. For both $\text{NO}^-(\text{N}_2\text{O})_1$ and $\text{NO}^-(\text{N}_2\text{O})_2$, the ion-solvent dissociation energies for the loss of single N_2O solvent molecules were determined from origin peak shifts to be ~ 0.2 eV. Electron affinities for $\text{NO}(\text{N}_2\text{O})_1$ and $\text{NO}(\text{N}_2\text{O})_2$ were determined to be 0.258 ± 0.009 eV and 0.513 ± 0.022 eV, respectively. The localization of the cluster ion's excess negative charge onto its nitric oxide rather than its nitrous oxide subunit was interpreted in terms of kinetic factors and a possible barrier between the two forms of the solvated ion.

$\text{H}^-(\text{NH}_3)_{n=1,2}$ The gas-phase $\text{H}^-(\text{NH}_3)_1$ ion was first observed by Nibbering⁴ in a FT-ICR spectrometer. Theoretical calculations by Rosmus, by Squires, by Schleyer, by Cremer, and by Ortiz all agree that the hydride ion is bound at a relatively long distance to only one of ammonia's hydrogens in the most stable configuration of the $\text{H}^-(\text{NH}_3)_1$ ion-dipole complex, and that $\text{H}^-(\text{NH}_3)_1$ is more stable than $\text{NH}_2^-(\text{H}_2)_1$. These

calculations found global minima for $\text{H}^-(\text{NH}_3)_1$ in which the H^- ion lies almost in line with a N-H bond in ammonia. Most of them also found values for the dissociation energy of $\text{H}^-(\text{NH}_3)_1$ into $\text{H}^- + \text{NH}_3$ that ranged around about a third of an eV.

In this work, $\text{H}^-(\text{NH}_3)_{n=1,2}$ ions were generated from ammonia in a supersonic expansion-ion source and photodetached with 2.540 eV photons.^{5,6} No homologous series in $\text{NH}_2^-(\text{H}_2)_n$ was observed. The photoelectron spectra of $\text{H}^-(\text{NH}_3)_1$ and $\text{H}^-(\text{NH}_3)_2$ are both dominated by large peaks which we have designated as peaks A and A', respectively, in Fig. 3. The $\text{H}^-(\text{NH}_3)_1$ spectrum also exhibits a smaller peak on the low electron kinetic energy side of peak A which we have labelled peak B. The shoulder on the low electron kinetic energy side of peak A' in the $\text{H}^-(\text{NH}_3)_2$ spectrum is marked in Fig. 3 as peak B'. A much smaller third peak (peak C) also exists in the $\text{H}^-(\text{NH}_3)_1$ spectrum. This will be discussed in a separate section below.

Our interpretation of peak A in the $\text{H}^-(\text{NH}_3)_1$ spectrum and of peak A' in the $\text{H}^-(\text{NH}_3)_2$ spectrum is that they contain the origins of their respective photodetachment transitions. Both peaks are due to the photodetachment of solvated hydride ion "chromophores" within $\text{H}^-(\text{NH}_3)_1$ and $\text{H}^-(\text{NH}_3)_2$. This results in the main features (peaks A and A') of the $\text{H}^-(\text{NH}_3)_1$ and $\text{H}^-(\text{NH}_3)_2$ photoelectron spectra resembling the photoelectron spectrum of free H^- (a single peak) except for being broadened and shifted to lower electron kinetic energies due to the stabilizing effect of solvation.

The electron binding energy of peak A is 1.11 eV. This is interpreted as an upper limit to the energy difference between the lower vibrational states of $\text{H}^-(\text{NH}_3)_1$ and the $\text{H} + \text{NH}_3 + \text{e}^-$ dissociation asymptote. This value is thus a reasonably close approximation to the dissociative detachment energy of $\text{H}^-(\text{NH}_3)_1$ [and to the electron affinity of $\text{H}(\text{NH}_3)$]. The electron binding energy of peak A' is 1.46 eV and it is similarly interpreted. An upper limit to the ion-solvent dissociation energy of $\text{H}^-(\text{NH}_3)_1$ into H^- and NH_3 (the gas-phase solvation energy) is given by subtracting the electron affinity of H (0.754 eV) from the value we have obtained for the upper limit to the dissociative detachment energy of $\text{H}^-(\text{NH}_3)_1$ ie. the origin peak shift. This value is 0.36 eV, and it is in very good agreement with theoretical calculations. Likewise, the ion-solvent dissociation energy of $\text{H}^-(\text{NH}_3)_2$ into $\text{H}^-(\text{NH}_3)_1$ and NH_3 is given by subtracting the dissociative detachment energy of $\text{H}^-(\text{NH}_3)_1$ from

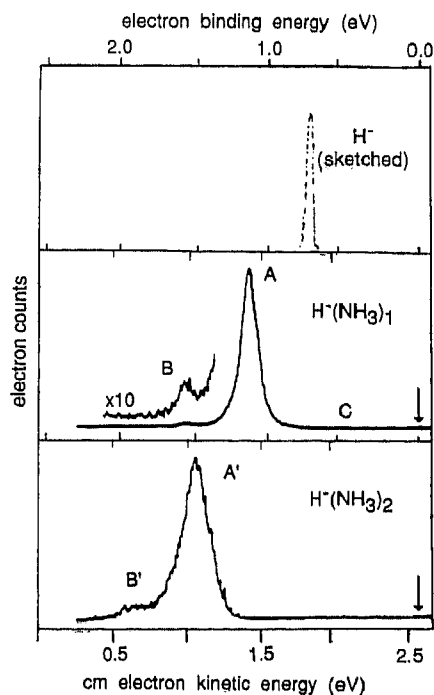


FIG. 3 The photoelectron spectra of $\text{H}^-(\text{NH}_3)_1$ and $\text{H}^-(\text{NH}_3)_2$. The spectrum of $\text{H}^-(\text{NH}_3)_1$ also shows a x30 magnified trace.

that of $\text{H}^-(\text{NH}_3)_2$ *ie.* the shift between these origin peaks. This value is 0.35 eV.

Our interpretation of peak B is that it is primarily due to the excitation of a stretching mode (or modes) in the ammonia solvent during photodetachment. The small Franck-Condon factor observed suggests that the ammonia solvent is only slightly distorted by its complexation with H^- . The center of peak B is separated from that of peak A by $3480 \pm 60 \text{ cm}^{-1}$ in the $\text{H}^-(\text{NH}_3)_1$ spectrum, and in the $\text{D}^-(\text{ND}_3)_1$ spectrum, the separation between the centers of peaks A and B is $2470 \pm 80 \text{ cm}^{-1}$. These peak separations are close to the observed stretching frequencies of NH_3 and ND_3 , and they therefore support our interpretation. The B' shoulder in the spectrum of $\text{H}^-(\text{NH}_3)_2$ is probably due to analogous transitions. Taken together, the foregoing provides spectroscopic evidence for cluster ions consisting of intact hydride ions which are perturbed and solvated by ammonia.

$\text{NH}_2^-(\text{NH}_3)_{n=1,2}$ Figure 4 presents the photoelectron spectra of NH_2^- , $\text{NH}_2^-(\text{NH}_3)_1$, $\text{NH}_2^-(\text{NH}_3)_2$ all plotted on a common center-of-mass electron kinetic energy scale.⁷ The well-known photoelectron spectrum of NH_2^- is dominated by a single peak, and it is presented in Figure 4 for comparative purposes. The spectra of the clustered ions are also dominated by large peaks (A and A'). These shift to lower electron kinetic energies with increasing solvation and are broadened. Our interpretation of peaks A and A' is that they both contain the origins of their respective photodetachment transitions. Both peaks arise due to the photodetachment of solvated amide ion "chromophores" within the $\text{NH}_2^-(\text{NH}_3)_1$ and $\text{NH}_2^-(\text{NH}_3)_2$ cluster ions. The spectral shifts are a consequence of the stabilization of the NH_2^- sub-ion due to its interactions with the NH_3 "solvent" molecule(s) in the cluster ions.

The center of peak A in the $\text{NH}_2^-(\text{NH}_3)_1$ spectrum corresponds to an electron binding energy of 1.30 eV. This is interpreted as an upper limit to the energy difference between the lower vibrational states of $\text{NH}_2^-(\text{NH}_3)_1$ and the $\text{NH}_2^- + \text{NH}_3 + e^-$ dissociation asymptote. This value is a close approximation to the dissociative detachment energy of $\text{NH}_2^-(\text{NH}_3)_1$, and to the electron affinity. The center of peak A' in the $\text{NH}_2^-(\text{NH}_3)_2$ spectrum corresponds to an electron binding energy of 1.78 eV, and it is similarly interpreted. An upper limit to the ion-solvent dissociation energy of $\text{NH}_2^-(\text{NH}_3)_1$ into NH_2^- and NH_3 (the gas-phase solvation energy) is given by the magnitude of the shift between the centers of the peak in the NH_2^- spectrum and peak A in the $\text{NH}_2^-(\text{NH}_3)_1$ spectrum. This is equivalent to subtracting our measured value for the electron affinity of NH_2^- from the value of the upper limit to the dissociative detachment energy of $\text{NH}_2^-(\text{NH}_3)_1$. This value is 0.52 eV, and it is in good agreement with theoretical calculations by Squires. Likewise, the ion-solvent dissociation energy of $\text{NH}_2^-(\text{NH}_3)_2$ into $\text{NH}_2^-(\text{NH}_3)_1$ and NH_3 is given by the shift between the centers of peaks A and A' in the cluster ion spectra. This value is 0.48 eV, indicating an approximately equal stabilization of NH_2^- by both the first and the second NH_3 "solvent" molecules.

A less intense peak, designated as peak B, appears on the low electron kinetic energy side of peak A in the photoelectron spectrum of $\text{NH}_2^-(\text{NH}_3)_1$. The separation between the centers of peaks A and B is close to the observed values of the stretching frequencies of ammonia. Our interpretation of this peak is that it is primarily due to the excitation of a stretching mode (or modes) in the NH_3 solvent during photodetachment. The photoelectron spectrum of $\text{ND}_2^-(\text{ND}_3)_1$ offers further

support of this interpretation. Peak A occurs at essentially the same location in the spectra of $\text{ND}_2^-(\text{ND}_3)_1$ and $\text{NH}_2^-(\text{NH}_3)_1$. The spacing between peaks A and B in the spectrum of $\text{ND}_2^-(\text{ND}_3)_1$, however, has decreased to an energy which is equal to the values of the observed stretching frequencies of ND_3 .

In previous photoelectron experiments on negative cluster ions, we have also studied the species, $\text{H}^-(\text{NH}_3)_1$ and $\text{H}^-(\text{NH}_3)_2$. Qualitatively the photoelectron spectra of $\text{NH}_2^-(\text{NH}_3)_{n=1,2}$ and $\text{H}^-(\text{NH}_3)_{n=1,2}$ are rather similar. Both sets of spectra exhibit large peaks (A and A' peaks). Both $\text{H}^-(\text{NH}_3)_1$ and $\text{NH}_2^-(\text{NH}_3)_1$ spectra have B peaks to the low electron energy side of their A peaks which are separated from them by energies corresponding to that of ammonia's stretching frequencies.

Quantitatively, however, the $\text{NH}_2^-(\text{NH}_3)_{n=1,2}$ spectra exhibit larger shifts and more broadening than the $\text{H}^-(\text{NH}_3)_{n=1,2}$ spectra. We have found that the first and second ion-solvent dissociation energies for $\text{NH}_2^-(\text{NH}_3)_1$ and $\text{NH}_2^-(\text{NH}_3)_2$ are both ~ 0.5 eV, while those for $\text{H}^-(\text{NH}_3)_1$ and $\text{H}^-(\text{NH}_3)_2$ are both ~ 0.35 eV. Clearly, the interaction of NH_2^- with ammonia is stronger than that of H^- with ammonia. Calculations by Squires find that $\text{H}^-(\text{NH}_3)_1$ and $\text{NH}_2^-(\text{NH}_3)_1$ have similar gross structures. Using flowing afterglow techniques to study the $\text{NH}_2^- + \text{H}_2 \rightarrow \text{H}^- + \text{NH}_3$ reaction, Bohme has shown that NH_2^- is a stronger base than H^- in the gas-phase. It thus seems likely that the higher ion-solvent dissociation energy of $\text{NH}_2^-(\text{NH}_3)_1$ relative to that of $\text{H}^-(\text{NH}_3)_1$ is a consequence of NH_2^- being a stronger base than H^- .

The clustering of solvent molecules around a bare gas-phase anion stabilizes the excess negative charge on the ion, and this results in a decrease in the gas-phase basicity. It is often the case, in fact, that the ordering of basicities in the gas-phase is the reverse of their ordering in solution. Using our results to calculate the relative basicities of NH_2^- vs H^- , $\text{NH}_2^-(\text{NH}_3)_1$ vs $\text{H}^-(\text{NH}_3)_1$, and $\text{NH}_2^-(\text{NH}_3)_2$ vs $\text{H}^-(\text{NH}_3)_2$ shows that such a reversal in the ordering of basicities in these systems occurs by the addition of a second ammonia solvent to NH_2^- and to H^- . This illustrates the role that cluster ions can play in illuminating the regime between the gaseous and the condensed (solution) phase.

Both $\text{NH}_2^-(\text{NH}_3)_1$ and $\text{H}^-(\text{NH}_3)_1$ spectra show an A-B peak spacing that is indicative of an ammonia stretching frequency. The relative intensity of the B peak in each of these spectra is a measure of the degree to which the ammonia "solvent" molecule is distorted due to its complexation with the anion. This peak is larger in the $\text{NH}_2^-(\text{NH}_3)_1$ spectrum than in the

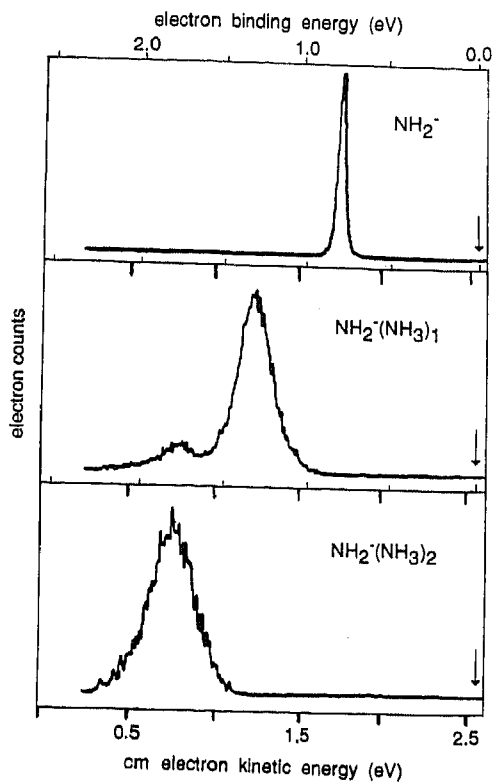


Fig. 4 The photoelectron spectra of NH_2^- , $\text{NH}_2^-(\text{NH}_3)_1$, and $\text{NH}_2^-(\text{NH}_3)_2$ all recorded with 2.540 eV photons.

$\text{H}^-(\text{NH}_3)_1$ spectrum, and this is consistent with the stronger interaction implied by the larger ion-solvent bond dissociation energy found for $\text{NH}_2^-(\text{NH}_3)_1$. These observations are also consistent with calculations by Squires. He finds that the ammonia N-H bond which interacts with the anion is more elongated in $\text{NH}_2^-(\text{NH}_3)_1$ than in $\text{H}^-(\text{NH}_3)_1$.

$\text{NO}^-(\text{Ar})_1$, $\text{NO}^-(\text{Kr})$, and $\text{NO}^-(\text{Xe})_1$ The photoelectron spectra of $\text{NO}^-(\text{Ar})_1$, $\text{NO}^-(\text{Kr})_1$, and $\text{NO}^-(\text{Xe})_1$ were recorded with 2.409 eV photons.⁸ All of these rare gas (Rg) negative cluster ion spectra exhibit structured spectral patterns which strongly resemble that obtained for free NO^- , but which are shifted to lower electron energies with their individual peaks broadened (see Figure 5). Each of these spectra is interpreted in terms of a largely intact NO^- sub-ion which is solvated and stabilized by its rare gas solvent atom. The ion-solvent

dissociation energy for a given $\text{NO}^-(\text{Rg})_1$ cluster ion dissociating into NO^- and Rg is approximately given by the energy difference between the origin peak of the free NO^- spectrum and the origin peak of a given $\text{NO}^-(\text{Rg})_1$ spectrum. The values of these shifts were found to be: 0.058 ± 0.011 eV, 0.099 ± 0.018 eV, 0.161 ± 0.024 eV for the argon, krypton, and xenon complexes, respectively. A plot of these energy shifts vs. the polarizabilities of the rare gas atoms gave a straight line. Values for the electron affinities of these complexes were found to be: 0.095 eV, 0.136 eV, and 0.204 eV for the argon, krypton, and xenon complexes, respectively.

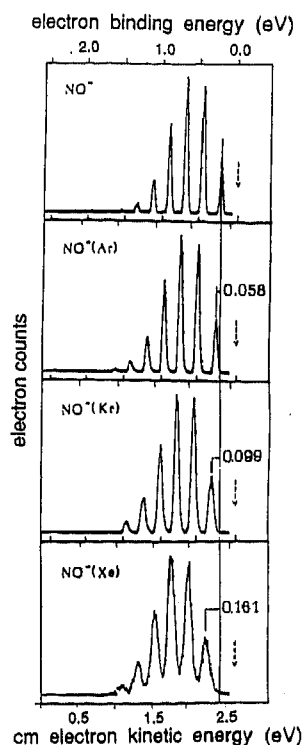


Fig. 5 The photoelectron spectra of NO^- , $\text{NO}^-(\text{Ar})_1$, $\text{NO}^-(\text{Kr})_1$, and $\text{NO}^-(\text{Xe})_1$

$\text{O}_2^-(\text{Ar})_1$ The photoelectron spectrum of $\text{O}_2^-(\text{Ar})_1$ exhibits the highly structured photoelectron spectral pattern of free O_2^- shifted to lower electron kinetic energy by ~ 70 meV, the ion-atom dissociation energy of

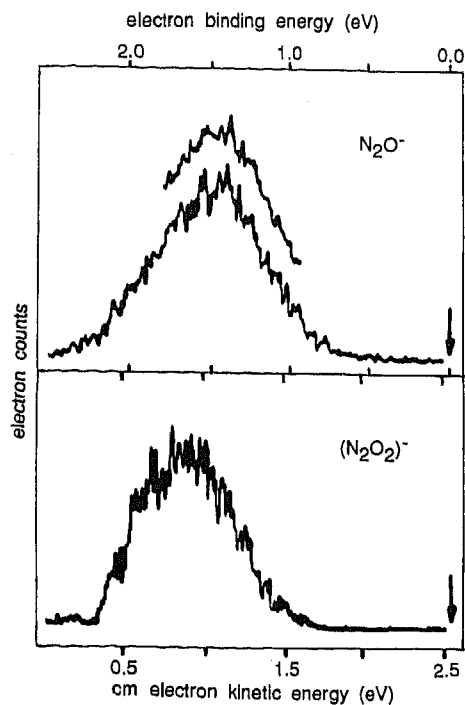


Fig. 6 The photoelectron spectrum of (a) N_2O^- and (b) $(\text{N}_2\text{O})_2^-$ presented in terms of center-of-mass electron kinetic energies and electron binding energies.

Both spectra were recorded with 2.540 eV photons.

The limited range scan above the full spectrum of N_2O^- has 2.5 times more signal.

this anion-complex. We are currently studying this system to see if an $\text{O}_2^-(\text{Ar})_1$ cluster ion with a vibrationally hot O_2^- component can survive the $\sim 10^{-5}$ sec flight time between the ion source and the laser interaction region without undergoing vibrational predissociation. If hot bands are observed in the $\text{O}_2^-(\text{Ar})_1$ spectrum, it will indicate that the vibrational predissociation lifetime is $> 10^{-5}$ sec.

N_2O^- and $(\text{N}_2\text{O})_2^-$ The photoelectron spectra of N_2O^- and $(\text{N}_2\text{O})_2^-$ were recorded with 2.540 eV photons⁹ (see Figure 6). Because of the large geometrical difference between N_2O (linear) and N_2O^- (bent), there is little Franck-Condon overlap between the lowest-lying levels in the ion and its neutral. We interpret the photoelectron spectrum of N_2O^- as

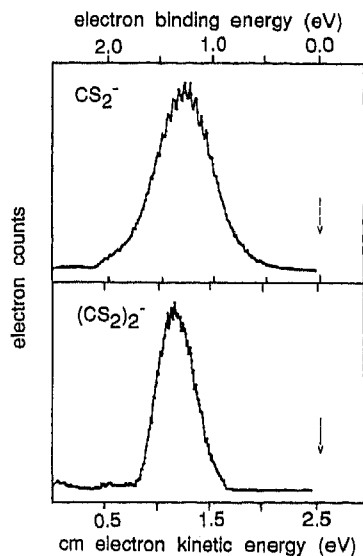


Fig. 7 The photoelectron spectra of the negative ions of carbon disulfide monomer and dimer are shown. The spectra were taken using 2.540 eV photons.

being largely due to an unresolved progression in the bending mode of N_2O . The electron binding energy corresponding to the maximum in the N_2O^- spectrum is ~ 1.5 eV and is a reasonable measure of the vertical detachment energy of N_2O^- . The spectrum of $(N_2O)_2^-$ provides information on the distribution of excess charge within the negative dimer ion. The maximum in the $(N_2O)_2^-$ spectrum is shifted by 0.19 eV to lower electron kinetic energy relative to the maximum in the N_2O^- spectrum. We interpret the $(N_2O)_2^-$ spectrum as arising from the photodetachment of an ionic species which is best described as a bent N_2O^- solvated by a neutral linear N_2O , *i.e.* as $N_2O^-(N_2O)_1$ and the ~ 0.2 eV shift between the N_2O^- and the $(N_2O)_2^-$ spectra as a measure of the dimer anion's dissociation energy into N_2O^- and N_2O .

$(CS_2)_2^-$ In addition to nitrous oxide, carbon disulfide and carbon dioxide are also linear triatomic molecules with bent anions. The photoelectron spectrum of $(CS_2)_2^-$ bears a substantial resemblance to that of the monomeric ion, CS_2^- (ref. 10), except for the former being shifted to lower electron energies relative to the latter (see Figure 7). Our interpretation of the $(CS_2)_2^-$ spectrum leads to the conclusion that $(CS_2)_2^-$ is composed of a largely intact CS_2^- ion which is "solvated" by a neutral

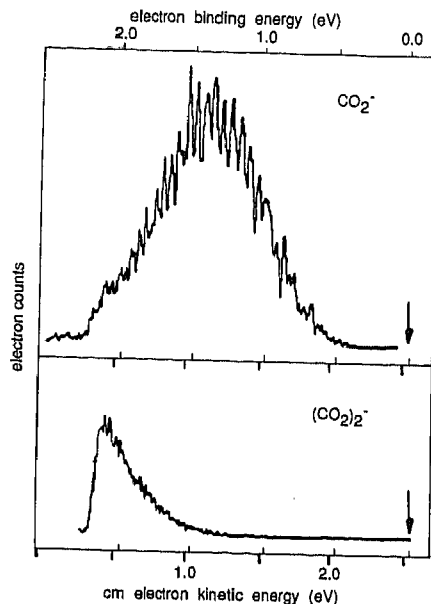


Fig. 8 The photoelectron spectra of (a) CO_2^- and (b) $(\text{CO}_2)_2^-$.

CS_2 , *ie.* the dimer ion is an ion-neutral complex. We have determined the ion-solvent dissociation energy for the dimer ion dissociating into CS_2^- and CS_2 to be 0.176 ± 0.025 eV.

More Complicated Cases: Cluster Anions with Excess Charge Dispersal

$(\text{CO}_2)_{n=1,2}^-$ The photoelectron spectra¹¹ of CO_2^- and $(\text{CO}_2)_2^-$, which were both recorded with 2.540 eV photons, are presented in Figure 8. Unlike N_2O and CS_2 , CO_2 has a negative adiabatic electron affinity. The negative ion, CO_2^- , is thus metastable and has an autodetachment lifetime of $\sim 10^{-4}$ sec. Because of the relative energies and large geometrical differences between CO_2 and CO_2^- , there should be no Franck-Condon overlap between the lowest lying levels of the ion and its neutral. We interpret the photoelectron spectrum of CO_2^- as being largely due to a progression in the bending mode of CO_2 . The structure near the maximum of the CO_2^- spectrum is real and the peak spacings probably correspond to the energy differences between anharmonic bending levels in CO_2 . The electron binding energy corresponding to the maximum in our CO_2^- spectrum can be associated with its vertical detachment energy. This value, 1.4 eV, is in good agreement with Jordan's calculated value for the vertical detachment energy of CO_2^- . The photoelectron spectrum of $(\text{CO}_2)_2^-$ is presented in Fig. 8b. The downward turn on the low electron kinetic energy side of this spectrum is an experimental artifact due to the rapid

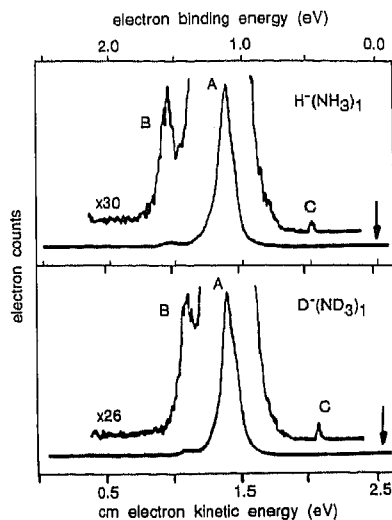


Fig. 9 The photoelectron spectra of $\text{H}^-(\text{NH}_3)_1$, $\text{D}^-(\text{ND}_3)_1$, $\text{NH}_4^-(\text{Td})$, and $\text{ND}_4^-(\text{Td})$.

and unavoidable decrease in the transmission functions of electron energy analyzers at low electron kinetic energies. Spectra taken with 2.707 eV photons show that the photodetachment cross section is still increasing at the false maximum in the 2.540 eV spectrum. Thus, with visible photons the spectrum of $(\text{CO}_2)_2^-$ exhibits only the lower energy photodetachment transitions of $(\text{CO}_2)_2^-$. Assuming that there is a spectral maximum in the $(\text{CO}_2)_2^-$ spectrum, it must occur at an electron binding energy that is >2.4 eV, *ie.* the maximum in the $(\text{CO}_2)_2^-$ spectrum is shifted to lower electron kinetic energies by >1 eV with respect to the maximum in the CO_2^- spectrum. This suggests that there is a substantial difference between $(\text{CO}_2)_2^-$ and $(\text{N}_2\text{O})_2^-$ and $(\text{CS}_2)_2^-$. Recent calculations by Jordan on the various possible structures for $(\text{CO}_2)_2^-$ shed substantial light on this problem. Upon reexamining the relative energies of the symmetrical D_{2d} form of C_2O_4^- and the asymmetrical ion-molecule complex, Jordan found the former to be more stable by ~ 0.2 eV. More importantly, however, he also found that these two forms of the anion gave very different vertical detachment energies, and that the calculated VDE for the D_{2d} form is in agreement with our measurements. Thus, it appears that even though $(\text{N}_2\text{O})_2^-$ and $(\text{CS}_2)_2^-$ are ion-molecule complexes, $(\text{CO}_2)_2^-$ is not. It is probably better described as C_2O_4^- .

NH_4^- As mentioned earlier, the photoelectron spectrum of NH_4^- is dominated by two peaks (A and B) which arise due to the photodetachment of electrons from the ion-molecule complex, $\text{H}^-(\text{NH}_3)_1$. In addition, however, there is also a much smaller third peak (C) in the spectrum, and

this feature provides the first experimental evidence for a higher energy isomer of NH_4^- of tetrahedral geometry.¹² Fig. 9 shows magnified traces of peak C in both the $\text{H}^-(\text{NH}_3)_1$ and the $\text{D}^-(\text{ND}_3)_1$ spectra. Since negative ions in this experiment are carefully mass-selected before photodetachment, the existence of peak C in both of these spectra is good evidence that it is not due to an "impurity" ion. Peak C occurs at too high of an electron kinetic energy to be due to NH_2^- (or to OH^-). Since clustering is expected to stabilize the excess negative charge on an anion and to shift spectral features toward lower (rather than higher) electron energies, it is also unlikely that peak C is due to the presence of small amounts of $\text{NH}_2^-(\text{H}_2)_1$. The photodissociation of $\text{H}^-(\text{NH}_3)_1$ into $\text{H}^- + \text{NH}_3$ followed by the photodetachment of electrons from the nascent H^- is a two-step process which is energetically-accessible with 2.5 eV photons. If this process were to occur, however, it would result in electrons with kinetic energies substantially lower than that of peak C (possible kinematic effects having been carefully considered). In addition, the laser power dependence of peak C's intensity is linear, and while not proof in itself, this is consistent with a single photon process. Further insight into the possible origin of peak C derives from its intensity variation with source conditions and from its behavior in the spectrum of the deuterated cluster ion, $\text{D}^-(\text{ND}_3)_1$. While the relative intensities of peaks A and B are essentially constant as source conditions are varied, the relative intensity of peak C changes substantially from day to day. Such intensity variations are indicative of photodetachment transitions which originate from an excited state of the ion and they are often associated with vibrationally-excited negative ion states. Hot band peaks arising from such transitions, however, should shift with deuteration, and peak C does not. Peak C behaves as if it arises from the photodetachment of an electronically higher energy form of the negative ion. It seems unlikely that peak C is due to the photodetachment of an electronically-excited state of $\text{H}^-(\text{NH}_3)_1$. Our observations are consistent with it being due to the photodetachment of a higher energy isomer of an ion with molecular formula, NH_4^- . The width of peak C is rather narrow, much narrower than peaks A and B. This implies that the structure of the ion being photodetached and the equilibrium structure of its corresponding neutral are rather similar. Neutral NH_4 is known to have a tetrahedral configuration. This suggests that the form of NH_4^- that gives rise to peak C is also of tetrahedral geometry. Also, the united atom for NH_4 is Na. The electron affinity of Na is ~0.5 eV. The electron binding energy of the species that gives rise to peak C is ~0.5 eV. In addition, calculations by Schleyer, by Cremer, and by

Ortiz all find a higher energy isomer of NH_4^- of tetrahedral geometry. The energy of $\text{NH}_4^-(T_d)$ above the global minima of $\text{H}^-(\text{NH}_3)_1$ is also consistent with our spectra. It seems likely that $\text{NH}_4^-(T_d)$ should be envisioned as an NH_4^+ core with two Rydberg-like electrons around it. Thus, NH_4^+ , NH_4 , and NH_4^- can all exist in tetrahedral forms. Moreover, they are all really the same thing ie. NH_4^+ cores with 0, 1, and 2 loose electrons associated with them.

$(\text{SO}_2)_2^-$ and $(\text{NO})_2^-$ The photoelectron spectra of $(\text{SO}_2)_2^-$ and of $(\text{NO})_2^-$ do not show the shifted "fingerprint" spectral patterns of SO_2^- and of NO^- that one might expect of simple, localized excess charge ion-molecule complexes^{13,14} ie. of $\text{SO}_2^-(\text{SO}_2)_1$ and of $\text{NO}^-(\text{NO})$. The component parts of these dimer ions may resonantly share the excess electron. This appears likely in the case of $(\text{SO}_2)_2^-$ where the observed spectral shift between the origin peak of the SO_2^- spectrum and the suspected origin in the $(\text{SO}_2)_2^-$ spectrum implies an ion-solvent dissociation energy that is reasonable for an ion-molecule complex. The spectrum of $(\text{NO})_2^-$, on the other hand, implies a lower limit to its electron affinity of ~ 2.1 eV. This implies that $(\text{NO})_2^-$ enjoys a high degree of electron dispersal, and that it may be better described as the unclustered ion, N_2O_2^- . Studies by Johnson¹⁵ at higher photon energies indicate the existence of other isomers of N_2O_2^- as well.

$\text{Na}_{n=2-5}^-$, $\text{K}_{n=2-8}^-$, $\text{Rb}_{n=2-4}^-$, and $\text{Cs}_{n=2,3}^-$ The study of metal clusters provides an avenue for exploring the variation in the electronic properties of metals in the transition size regime between atoms and the solid state bulk. For metals, properties such as ionization potentials and electron affinities typically vary in magnitude by several eV from their atomic to their bulk (work function) values. Presumably, clusters of intermediate size have electronic properties of intermediate values. For phenomena where the properties of matter in the regime of small sizes are important, eg. surface reactivity and thin films, these variations in electronic properties can have pivotal effects. In principle, the study of the electronic properties of metal clusters as a function of cluster size could allow us to observe the evolution of the electronic states of metals from those of their atoms to those of band theory.

The alkali metals are the simplest of metals. We have recently recorded the photoelectron spectra of $\text{Na}_{n=2-5}^-$, $\text{K}_{n=2-8}^-$, $\text{Rb}_{n=2-4}^-$, and $\text{Cs}_{n=2,3}^-$ using 2.540 eV photons (see Fig. 10).¹⁶ These highly structured spectra map out both the electron affinities vs cluster size for those cluster anions studied thus far and the electronic state splittings of

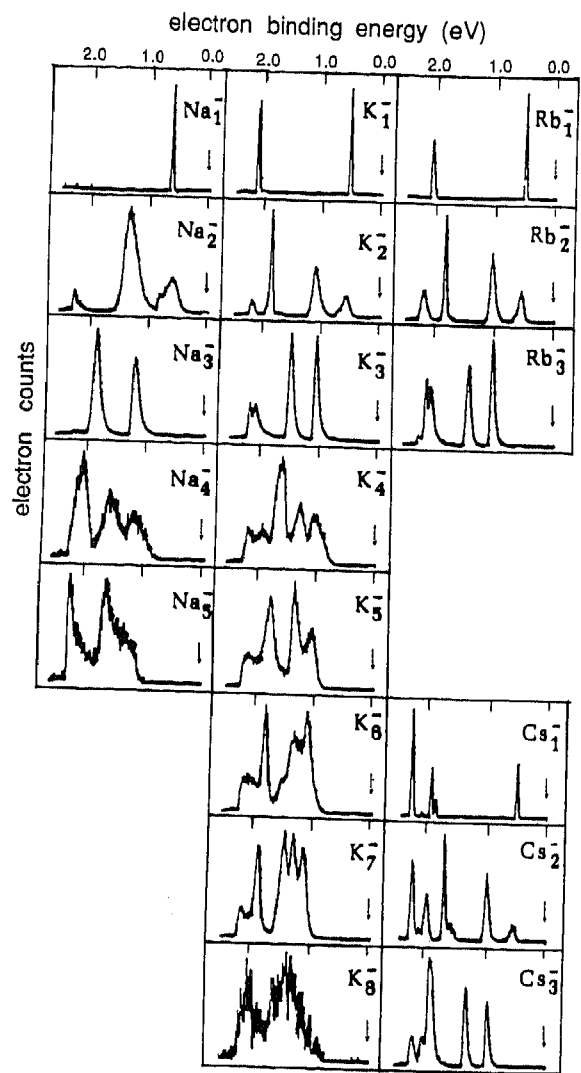


Fig. 10 The Photoelectron Spectra of Alkali Metal Cluster Anions

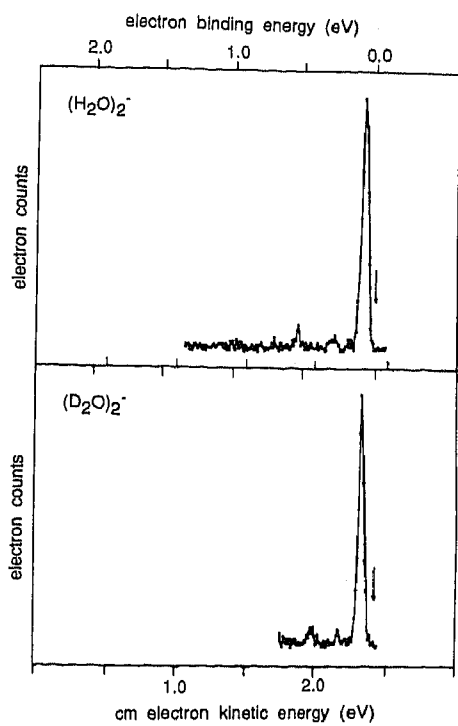


Fig. 11 The photoelectron spectra of $(\text{H}_2\text{O})_2^-$ and $(\text{D}_2\text{O})_2^-$

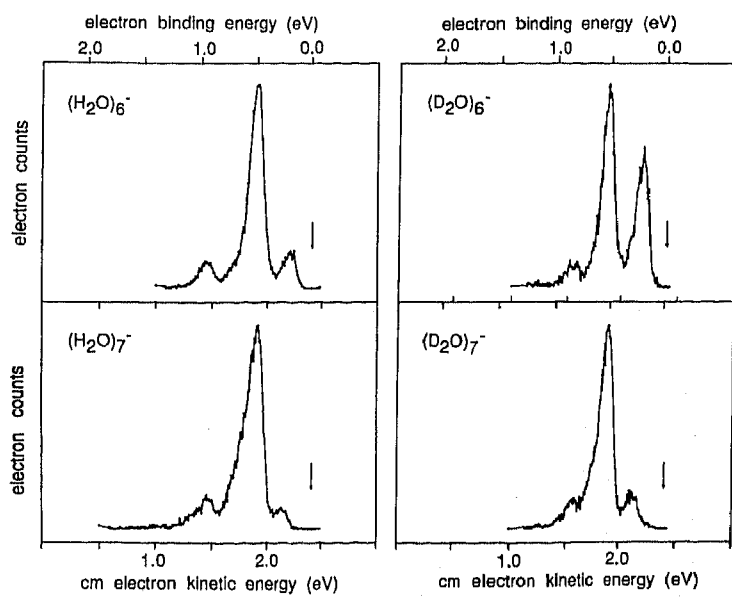


Fig. 12 The photoelectron spectra of $(\text{H}_2\text{O})_{6,7}^-$ and $(\text{D}_2\text{O})_{6,7}^-$

their corresponding neutral clusters (at the geometry of their cluster anions) vs cluster size. The dimer anion spectra have been completely assigned. These provide adiabatic electron affinities, vertical detachment energies, dimer anion dissociation energies, neutral dimer electronic state spacings, and bond lengths for the various excited electronic states of the neutral dimers. Thus far, we have obtained our most complete set of data on potassium cluster anions. Potassium ($[\text{Ar}]4s^1$) should be electronically analogous to copper ($[\text{Ar}]3d^{10}4s^1$). A comparison of the electron affinity vs cluster size trends for potassium clusters with those for copper clusters (measured by Lineberger¹⁷ and by Smalley¹⁸) of the same size, shows quantitative differences (copper has a substantially larger work function) yet strikingly similar qualitative trends. Most of the structure in these spectra comes about due to the electronic states of the neutral clusters. One can see qualitative similarities between the UV photodetachment spectra of copper cluster anions and our visible spectra of potassium cluster anions. This correlation with the UV experiments is reasonable since the electronic states of neutral copper clusters might be expected to be more widely spaced in energy than those of neutral potassium clusters.

$(\text{H}_2\text{O})_{n=2,6,7,10-17,19}^-$ and $\text{Ar}(\text{H}_2\text{O})_{n=2,6,7}^-$ Over the years, it has often been suggested that gas-phase $(\text{H}_2\text{O})_n^-$ cluster ions ought to exist, and that they might be gas-phase counterparts to condensed phase solvated (hydrated) electrons. A few years ago, these entities were observed for the first time in the gas-phase by Haberland.

Recently, we generated $(\text{H}_2\text{O})_{n=11-21}^-$ from neat water expansions in a supersonic expansion ion source and recorded the photoelectron spectra of $(\text{H}_2\text{O})_{n=11-15,19}^-$ using 2.409 eV photons.¹⁹ Each of these spectra consists of a single broadened peak, and these are shifted to successively lower electron kinetic energies with increasing cluster ion size. We interpreted the electron binding energies of the fitted centers of these spectral peaks to correspond to the vertical detachment energies for each of the cluster anions. These vertical detachment energies vary smoothly from 0.75 eV for $(\text{H}_2\text{O})_{11}^-$ to 1.12 eV for $(\text{H}_2\text{O})_{19}^-$.

Currently, we are collaborating with H. Haberland and his student, C. Ludewigt to photodetach more water cluster anions. Thus far, we have looked at $(\text{H}_2\text{O})_{2,6,7}^-$ and $(\text{D}_2\text{O})_{2,6,7}^-$ [see Figure 11 and 12]; and $\text{Ar}(\text{H}_2\text{O})_{2,6,7}^-$ and $\text{Ar}(\text{D}_2\text{O})_{2,6,7}^-$. We plan to extend these studies to much larger cluster anions in the near future.

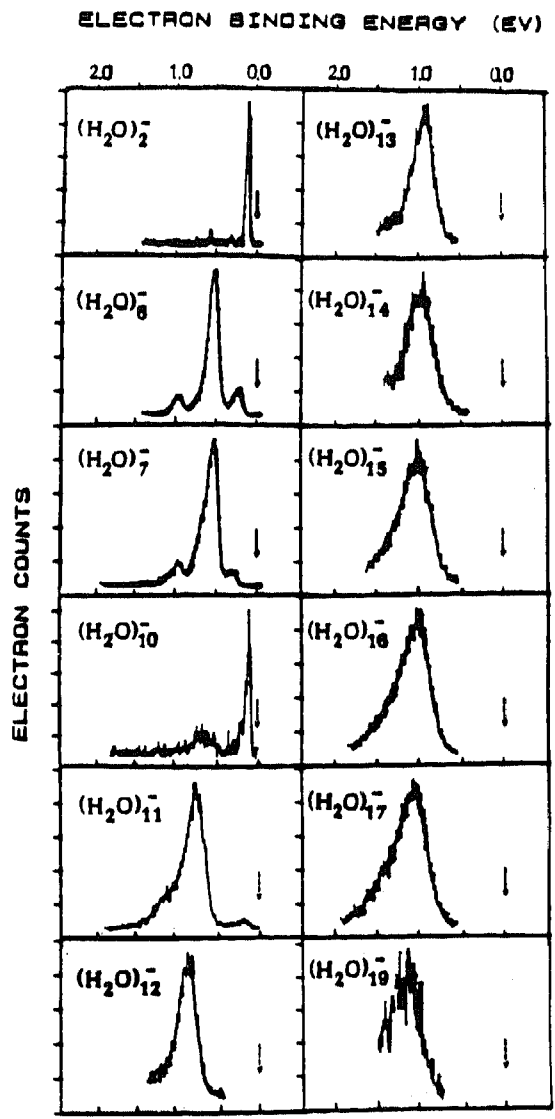


Fig. 13 The Photoelectron Spectra of $(\text{H}_2\text{O})_{n=2,6,7,10-17,19}^-$

The spectrum of the water dimer anion is particularly interesting. Calculations have generally predicted the structure of $(\text{H}_2\text{O})_2^-$ to be the same as that of $(\text{H}_2\text{O})_2$, *i.e.*, the excess electron was not found to distort the structure of neutral water dimer. In the spectrum of $(\text{H}_2\text{O})_2^-$, however, we observe peak spacings which are characteristic of H_2O bending and H_2O stretching frequencies. In the $(\text{D}_2\text{O})_2^-$ spectrum, we see these spacings shift appropriately for a D_2O bend and a D_2O stretch. Thus, it is reasonably clear that at least one water component within the water dimer anion is distorted! We also measure the vertical detachment energy to be ~ 34 meV for water dimer anion. Since there is at least some structural difference between the anion and its neutral, the adiabatic electron affinity of water dimer must be at least a little less than 34 meV. The field detachment experiments of Haberland determined the electron binding energy of $(\text{H}_2\text{O})_2^-$ to be ~ 17 meV. Figure 13 presents the photoelectron spectra of all of the $(\text{H}_2\text{O})_n^-$ species that we have studied thus far.

ACKNOWLEDGEMENTS

This research was supported by the National Science Foundation under Grant No. CHE-8511320. Some of the work on the negative cluster ions of water was performed in collaboration with H. Haberland, C. Ludewigt, and D. Worsnop, and was partially supported by a NATO Collaborative Research Grant (#86/307).

REFERENCES

1. J. V. Coe, J. T. Snodgrass, C. B. Freidhoff, K. M. McHugh, and K. H. Bowen, *J. Chem. Phys.* **84**, 618 (1986).
2. H. Haberland, H.-G. Schindler, and D. R. Worsnop, *Ber. Bunsenges. Phys. Chem.* **88**, 270 (1984).
3. J. V. Coe, J. T. Snodgrass, C. B. Freidhoff, K. M. McHugh, and K. H. Bowen, *J. Chem. Phys.* **87**, 4302 (1987).
4. J. C. Kleinfeld, S. Ingemann, J. E. Jalonen, N. M. M. Nibbering, *J. Am. Chem. Soc.* **105**, 2474 (1983).
5. J. V. Coe, J. T. Snodgrass, C. B. Freidhoff, K. M. McHugh, and K. H. Bowen, *J. Chem. Phys.* **83**, 3169 (1985).
6. J. T. Snodgrass, J. V. Coe, C. B. Freidhoff, K. M. McHugh, and K. H. Bowen, to be published.
7. J. T. Snodgrass, J. V. Coe, C. B. Freidhoff, K. M. McHugh, and K. H. Bowen, to be published.
8. C. B. Freidhoff, J. T. Snodgrass, and K. H. Bowen, to be published.
9. J. V. Coe, J. T. Snodgrass, C. B. Freidhoff, K. M. McHugh, and K. H. Bowen, *Chem. Phys. Lett.* **124**, 274 (1986).
10. J. M. Oakes and G. B. Ellison, *Tetrahedron* **42**, 6263 (1986).
11. J. V. Coe, Ph.D. Thesis, The Johns Hopkins University, 1986.
12. J. T. Snodgrass, Ph.D. Thesis, The Johns Hopkins University, 1987.
13. J. T. Snodgrass, J. V. Coe, C. B. Freidhoff, K. M. McHugh, and K. H. Bowen, submitted.

14. C. B. Freidhoff, Ph.D. Thesis, The Johns Hopkins University, 1987.
15. M. Johnson (private communication).
16. K. M. McHugh, J. G. Eaton, G. H. Lee, H. Sarkas, L. Kidder, and K. H. Bowen, to be published.
17. D. G. Leopold, Joe Ho, and W. C. Lineberger, *J. Chem. Phys.* 86, 1715 (1987).
18. O. Cheshnovsky, P. F. Brucat, S. Yang, C. L. Pettiette, M. J. Craycraft, and R. E. Smalley, Proceedings of the International Symposium on the Physics and Chemistry of Small Clusters, Richmond, VA, Oct. 28-Nov. 1, 1986.
19. J. V. Coe, D. Worsnop, and K. H. Bowen, submitted.